Additive Assembly for PolyJet-Based Multi-Material 3D Printed Microfluidics

Elizabeth H. Childs, Andrew V. Latchman, Andrew C. Lamont, Joshua D. Hubbard, and Ryan D. Sochol

***Abstract*— PolyJet-based additive manufacturing (or "three-dimensional (3D) printing") techniques allow for micro-to-mesoscale fluidic systems to be produced with multiple, fully integrated materials and unparalleled geometric versatility (due to the use of sacrificial support materials). Although the PolyJet 3D printing process is autonomous and fast, the post-processing methods required to remove the sacrificial materials can be exceedingly time-intensive for systems with enclosed channels, often resulting in device degradation. To bypass such issues, here we present a novel "additive assembly" strategy for realizing PolyJet-printed multi-material microfluidic components. In this work, we print a microfluidic capacitor as two separate halves to enable facile support material removal, and then fasten the parts together *via* designed integration features. Fabrication results revealed a significant reduction in post-processing time by approximately 98% compared to enclosed control designs. Experimental results for burst-pressure testing – a measure of component integrity – revealed that the additively assembled microfluidic capacitors retained a maximum internal pressure in excess of 189 kPa before failure. The results suggest that the presented additive assembly strategy holds promise for greatly extending the utility of PolyJet 3D printing for micro- and millifluidic applications. [2020-0111]**

***Index Terms*— Additive manufacturing, 3D printing, PolyJet, MultiJet, microfluidics.**

I. Introduction

ADDITIVE manufacturing (or colloquially, "three-dimensional (3D) printing") technologies have garnered increasing interest in the microfluidics community [1]–[3]. Motivated by the potential to circumvent the time, labor, and cost demands associated with conventional clean room-based microfluidics manufacturing [4] while greatly expanding the design flexibility [5], researchers have investigated alternatives in the form of additive manufacturing [6]. A number of groups have reported the construction of microfluidic systems using extrusion/nozzle [7], stereolithography [8], [9], direct laser writing [10], and MultiJet/PolyJet-based approaches [11]. Among these technologies, PolyJet printing – an inkjet-based process in which droplets of photomaterial (and sacrificial support material) are dispensed to produce 3D objects line-by-line, layer-by-layer – offers the highest versatility both in terms of design complexity and multi-material integration [12], [13]. Unfortunately, for microfluidic systems, removing sacrificial support material from enclosed microchannels can be exceedingly time and labor intensive [14], [15]. Thus, new strategies that bypass the challenges associated with support removal for microfluidic systems are in critical demand [16].

Recently, Yim *et al.* presented an "additive folding" approach in which the cross sections corresponding to each layer slice of a 3D design were cut out of a 2D elastic film, and then afterward, the layers were folded (or stacked) atop one another, ultimately producing a 3D object [17]. In this work, we explore the potential to adapt the additive folding concept to limit the support material removal difficulties associated with PolyJet-based microfluidics manufacturing. Using our previously presented multi-material microfluidic capacitor concept as an exemplar [18], we experimentally investigate the efficacy of a novel "additive assembly" strategy for enabling PolyJet 3D printing of multi-material microfluidic systems.

II. Concept

The additive assembly methodology in this work consists of five key steps. First, a 3D model of a microfluidic system is sectioned into separated components such that any and all internal channels become unenclosed. For example, an enclosed microfluidic capacitor [18] would be divided into two unenclosed halves. Second, multi-material features (*e.g.*, that promote flexible-to-rigid interactions akin to O-rings) and fastener elements are added along critical points of desired fluidic sealing. Third, the resulting parts are PolyJet 3D printed with the unenclosed channels facing upward, such that the sacrificial (*i.e.*, water-soluble) support material is never deposited into the unenclosed channels (Fig. 1a). Next, the water-soluble support material is removed from the parts (Fig. 1b). Lastly, the fasteners with string-like extrusions – all printed in place (Fig. 1a,b) – are used to align the parts and then tightly seal the final assembly (Fig. 1c). Thereafter, the part can be used for microfluidic operations. In this case, applied fluidic pressures result in the flexible diaphragm expanding (Fig. 1d) to store fluid volume (analogous to the ability for an electronic capacitor to store charge under an applied voltage).

III. Materials & Methods

Components in this work were modeled using the computer-aided design (CAD) software, SolidWorks (Dassault Systemes, France). The microfluidic capacitor was designed to yield rigid inlet/outlet channels (radii = 500 μm) connected to dual compliant diaphragms (thickness and separation distance = 1 mm). The models were exported as two STL files – *i.e.*, corresponding to the flexible and rigid materials

Manuscript received May 1, 2020; revised June 9, 2020; accepted June 17, 2020. Date of publication July 1, 2020; date of current version October 7, 2020. Subject Editor R. Ghodssi. *(Corresponding author: Ryan D. Sochol.)*

Elizabeth H. Childs, Andrew V. Latchman, Andrew C. Lamont, and Ryan D. Sochol are with the Department of Mechanical Engineering, University of Maryland, College Park, MD 20742 USA, and also with the Fischell Department of Bioengineering, University of Maryland, College Park, MD 20742 USA (e-mail: rsochol@umd.edu).

Joshua D. Hubbard is with the Department of Chemical and Biomolecular Engineering, University of California at Berkeley, Berkeley, CA 94720 USA.

Color versions of one or more of the figures in this article are available online at http://ieeexplore.ieee.org.

Digital Object Identifier 10.1109/JMEMS.2020.3003858

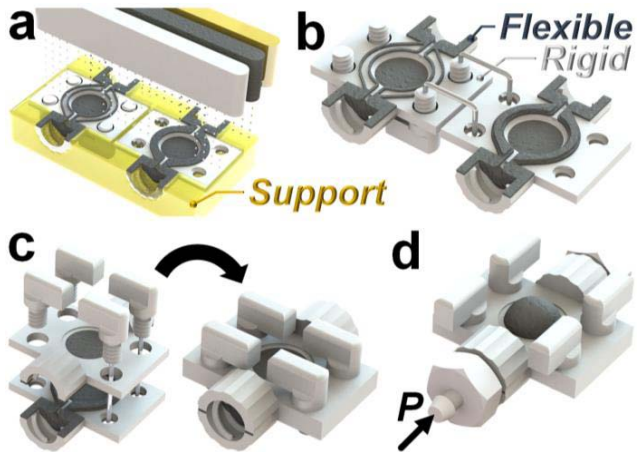

Fig. 1. Conceptual illustrations of the "additive assembly" strategy for manufacturing a multi-material microfluidic capacitor. (a) PolyJet 3D printing of flexible (*black*), rigid (*white*), and sacrificial support material (*yellow*). (b) Printed components following support material removal. (c) Assembly process. (d) An applied input pressure (P) results in diaphragm expansion.

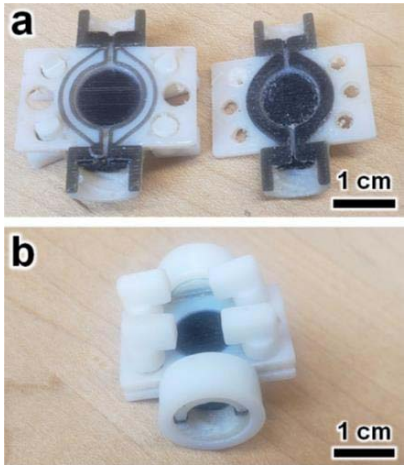

Fig. 2. Fabrication results for PolyJet 3D printing-based additive assembly. (a) Printed components following support material removal. *Black Material* = Agilus30 (*Flexible*); *White Material* = VeroWhite (*Rigid*); Fastener extrusions removed. (b) Microfluidic capacitor following the additive assembly process.

(support material is generated automatically by the printer software). The STL files were imported into the computer-aided manufacturing (CAM) software, GrabCAD Print (Stratasys, Eden Prairie, MN), and then printed with the Stratasys Objet500 Connex3 PolyJet 3D printer (print time $\approx$ 1-1.5 hr) using: (*i*) Agilus30 for the flexible material, (*ii*) VeroWhite for the rigid material, and (*iii*) SUP706 for the water-soluble support material (Stratasys). Following the PolyJet 3D printing process, parts were detached from the build plate, adherent support material was primarily removed manually, and then the parts were submerged in a solution of 2% sodium hydroxide and 2% sodium metasilicate (w/w) in DI water for 2 hr to remove any remaining support material. After drying, the parts were aligned and assembled manually (*i.e.*, by eye/hand) using the printed fasteners (*i.e.*, turning the printed screws until sensing resistance), while printed rings were placed around the ports (total post-processing time $\approx$ 2.5 hr).

Burst-pressure testing was performed using the Fluigent Microfluidic Control System (MFCS) and MAESFLO software (Fluigent, France). Input pressures were applied through fluorinated ethylene propylene tubing (Cole-Parmer, Vernon Hills, IL) connected to MFCS-LP Female Luer Connectors interfaced with the devices. Pressure was applied through one inlet port of each device, while the outlet port was blocked. During testing with pressurized air, devices with identical designs, printing, and post-processing protocols were submerged in water and monitored for visual indications of leaks while the input pressure was increased by: (*i*) 10 kPa increments up to 60 kPa, (*ii*) 5 kPa increments up to 90 kPa, (*iii*) 1 kPa increments up to 100 kPa, and (*iv*) 0.1 kPa increments thereafter (*i.e.*, until observed device failure). Following instances of leakage, the fasteners were retightened by hand (without any additional modifications) prior to initiating a subsequent trial.

IV. Results and Discussion

We initially investigated differences in the fabrication process with respect to printing enclosed microfluidic components. For the PolyJet 3D printing process, devices are fabricated in a line-by-line, layer-by-layer manner such that increases in part height correspond to significantly longer print times, whereas increases in print area for a particular layer do not affect the total print time as significantly. In this work, the PolyJet 3D printer was set to layer heights of 30 μm, which resulted in faster print times for the unenclosed halved sections compared to their taller enclosed counterparts (print time $\approx$ 2-2.5 hr) [18]. It should be noted that due to multiple initial layers of support material printed as a raft, the print time was reduced, but not fully by half as would be expected. We observed that the support removal process, however, was dramatically reduced (*i.e.*, by approximately 98%) compared to the four-day passive removal protocol required for the enclosed device [18].

To investigate the sealing efficacy of the additive assembly strategy, we aligned the distinct PolyJet-printed parts (Fig. 2a), assembled them into a singular component using the printed fasteners (Fig. 2b), and performed burst-pressure experiments with three distinct devices. Once assembled, the microfluidic capacitor design results in visible inflation of the flexible diaphragm under an applied input pressure (Fig. 3a). For the burst pressure test, each device was submerged in water (Fig. 3b) and monitored for two types of failure modes resulting in visible leakage (*i.e.*, air bubble generation): (*i*) assembly-associated leakage (from locations where the two distinct parts interact), and (*ii*) diaphragm leakage/fracture, which is unrelated to the additive assembly process. Experimental results for the first device initially revealed effective assembly integrity for pressures up to 134 kPa; however, subsequent trials failed at lower pressures of 90 kPa and then 98 kPa (Fig. 1c). A second device first exhibited assembly-based leakage at a slightly lower pressure of 116 kPa, but then maintained assembly integrity until one of the diaphragms failed at 111 kPa during the second trial (Fig. 1c). Experiments with a third device did not reveal any failures due to the additive assembly process as the device maintained internal pressures in excess of 189 kPa at which point a diaphragm ruptured (Fig. 1c). Despite differences in designs and printed material properties, the additive assembly results correspond to comparable and/or higher pressures than those reported in

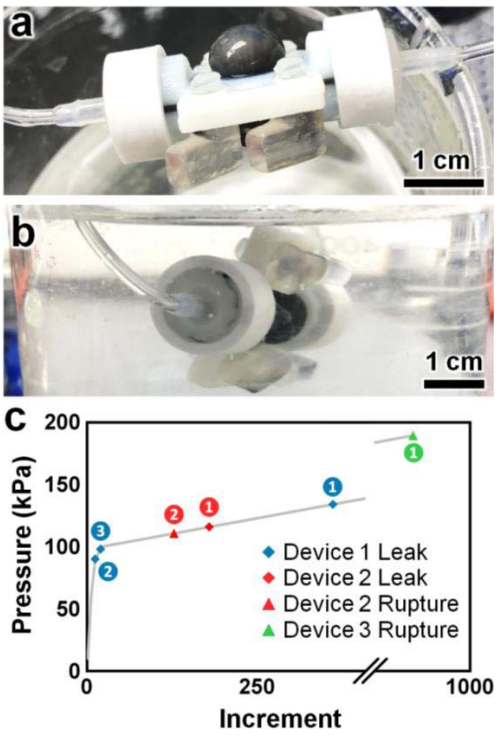

Fig. 3. Experimental results for additively assembled PolyJet 3D printing-based microfluidic capacitors. (a) Diaphragm expansion due to an applied input pressure. (b) Burst-pressure testing setup of device under water with applied pressurized air. (c) Quantified burst-pressure results for incremental increases in applied pressure. Markers denote: (*diamonds*) leaks in additively assembled interactions, (*triangles*) ruptures of the diaphragm, and (*numbers*) trial order.

prior works for fully enclosed inkjet-printed 3D microfluidic capacitors [15], [18].

V. Conclusion

PolyJet 3D printing offers unique capabilities for microfluidics design and manufacturing; however, the challenges associated with removing the required sacrificial support material from enclosed channels has represented a critical barrier to adoption. In this work, we presented and investigated a new strategy, termed additive assembly, as a means to bypass support material removal difficulties. Although the time associated with the PolyJet printing process was decreased (*i.e.*, due to the smaller height of the print), the significant benefit of this strategy was the vast reduction in the post-processing time typically required for passively dissolving the sacrificial support material out of enclosed channels [18]. One caveat, however, is that additional time was required to manually assemble the components. In addition, such manual protocols may have contributed to the relatively high degree of variability in the burst-pressure performance of the additively assembled components tested in the current study (Fig. 3c). Similar to the way in which the outcomes of multi-layer soft lithography protocols can be dependent on user skill and experience [12], so too do we expect user-related capabilities to influence additive assembly efficacy. A possible added benefit of limiting the amount of time during which the PolyJet-printed materials interact with the sodium hydroxide-sodium metasilicate support removal solution is that component materials may retain higher integrity (*e.g.*, by preventing material degradation from overexposure to the solution); however, future studies are needed to examine this prospect. Nonetheless, the high pressures at which assembled components were able to remain fluidically sealed (*e.g.*, with cases of the printed material fracturing prior to the assembly) suggest promise for the presented methodology for micro/millifluidics manufacturing. Thus, the additive assembly strategy presented here could enable new applications for lab-on-a-ship and soft robotic technologies.

Acknowledgment

The authors greatly appreciate the help and support of the members of the Bioinspired Advanced Manufacturing (BAM) Laboratory and the technical staff of Terrapin Works at the University of Maryland, College Park.

References

[1] F. Cecil, R. M. Guijt, A. D. Henderson, M. Macka, and M. C. Breadmore, "One step multi-material 3D printing for the fabrication of a photometric detector flow cell," *Analytica Chim. Acta*, vol. 1097, pp. 127–134, Feb. 2020.

[2] E. K. Parker *et al.*, "3D printed microfluidic devices with immunoaffinity monoliths for extraction of preterm birth biomarkers," *Anal. Bioanal. Chem.*, vol. 411, no. 21, pp. 5405–5413, Aug. 2019.

[3] A. P. Kuo, N. Bhattacharjee, Y. Lee, K. Castro, Y. T. Kim, and A. Folch, "High-precision stereolithography of biomicrofluidic devices," *Adv. Mater. Technol.*, vol. 4, no. 6, Jun. 2019, Art. no. 1800395.

[4] A. K. Au, W. Huynh, L. F. Horowitz, and A. Folch, "3D-printed microfluidics," *Angew. Chem. Int. Ed.*, vol. 55, no. 12, pp. 3862–3881, 2016.

[5] A. T. Alsharhan, R. Acevedo, R. Warren, and R. D. Sochol, "3D microfluidics via cyclic olefin polymer-based *in situ* direct laser writing," *Lab Chip*, vol. 19, no. 17, pp. 2799–2810, 2019.

[6] N. Bhattacharjee, A. Urrios, S. Kang, and A. Folch, "The upcoming 3D-printing revolution in microfluidics," *Lab Chip*, vol. 16, no. 10, pp. 1720–1742, 2016.

[7] M. A. Skylar-Scott *et al.*, "Biomanufacturing of organ-specific tissues with high cellular density and embedded vascular channels," *Sci. Adv.*, vol. 5, no. 9, Sep. 2019, Art. no. eaaw2459.

[8] Y. T. Kim, S. Bohjanen, N. Bhattacharjee, and A. Folch, "Partitioning of hydrogels in 3D-printed microchannels," *Lab Chip*, vol. 19, no. 18, pp. 3086–3093, 2019.

[9] H. Gong, A. T. Woolley, and G. P. Nordin, "3D printed selectable dilution mixer pumps," *Biomicrofluidics*, vol. 13, no. 1, Jan. 2019, Art. no. 014106.

[10] A. C. Lamont, A. T. Alsharhan, and R. D. Sochol, "Geometric determinants of *in-situ* direct laser writing," *Sci. Rep.*, vol. 9, no. 1, pp. 1–12, Dec. 2019.

[11] F. Zhu, J. Skommer, N. P. Macdonald, T. Friedrich, J. Kaslin, and D. Wlodkowic, "Three-dimensional printed millifluidic devices for zebrafish embryo tests," *Biomicrofluidics*, vol. 9, no. 4, Jul. 2015, Art. no. 046502.

[12] R. D. Sochol *et al.*, "3D printed microfluidics and microelectronics," *Microelectronic Eng.*, vol. 189, pp. 52–68, Apr. 2018.

[13] N. W. Bartlett *et al.*, "A 3D-printed, functionally graded soft robot powered by combustion," *Science*, vol. 349, no. 6244, pp. 161–165, Jul. 2015.

[14] N. P. Macdonald, J. M. Cabot, P. Smejkal, R. M. Guijt, B. Paull, and M. C. Breadmore, "Comparing microfluidic performance of three-dimensional (3D) printing platforms," *Anal. Chem.*, vol. 89, no. 7, pp. 3858–3866, Apr. 2017.

[15] R. D. Sochol *et al.*, "3D printed microfluidic circuitry via multijet-based additive manufacturing," *Lab Chip*, vol. 16, no. 4, pp. 668–678, 2016.

[16] A. D. Castiaux, C. W. Pinger, E. A. Hayter, M. E. Bunn, R. S. Martin, and D. M. Spence, "PolyJet 3D-printed enclosed microfluidic channels without photocurable supports," *Anal. Chem.*, vol. 91, no. 10, pp. 6910–6917, May 2019.

[17] S. Yim, C. Sung, S. Miyashita, D. Rus, and S. Kim, "Animatronic soft robots by additive folding," *Int. J. Robot. Res.*, vol. 37, no. 6, pp. 611–628, May 2018.

[18] J. D. Hubbard, C. Manny, A. Montgomery, B. Freeman, A. Boyle, and R. D. Sochol, "Multi-Material 3D Printed Microfluidic Circuitry Elements," in *Proc. 21st Int. Conf. Miniaturized Syst. Chem. Life Sci.*, Savannah, GA, USA, 2017, pp. 31–32.